From Quaternions to Non-Associative Octonionic Fields:
Modeling Dynamic Chemical Transformations and Thermodynamic Phase Shifts

Richard L. Lewis, PhD, AuG
Independent Researcher

SECTION 1. INTRODUCTION

This is the fourth in a series of interrelated papers exploring the possibility that hypercomplex numbers can usefully model biochemistry mathematically.

1.1 Sequence

In the first in the series, we established the spacetime quaternion framework $q = t + xi + yj + zk$ and its success in modeling static carbon sp3 tetrahedral geometry. We concluded that the application of hypercomplex algebra to molecular geometry provides a rigorous, secular, and computationally unified framework for analyzing organic structures.

In the second paper, we extended the hypercomplex scalar-body / vector-mind framework from abstract structural dualities to concrete molecular physics, specifically modeling the asymmetric geometry of the water molecule. While highly symmetric systems like methane obscure internal directional dynamics, the permanent dipole moment and lone-pair distributions of water provide an ideal validation environment for hypercomplex mechanics. We were able to show that setting hypercomplex spatial torques to zero resolves into a stable structural equilibrium that naturally predicts the empirical 104.5° molecular bond angle of water, offering a highly streamlined geometric alternative to conventional matrix-heavy quantum chemistry calculations.

1.2 The Limits of Quaternion Algebra

Quaternions excel at tracking 3D space, rotation, and single-particle states. However, when modeling active chemical changes, we encounter two major limitations:

The Dimensionality Limit (Degrees of Freedom): A single quaternion has 4 dimensions (1 scalar, 3 vectors). A chemical reaction involves position, momentum, electron spin, and energy states simultaneously. Four dimensions quickly become crowded, forcing you to stack multiple quaternions awkwardly.

The Commutativity of Fields: While quaternions are non-commutative ($\mathbf{ij} \neq \mathbf{ji}$), they are still associative ($a(bc) = (ab)c$). Quantum field changes and complex particle interactions often violate associativity when multiple overlapping states interfere with one another.

Quaternions excel at 3D tracking but lack the degrees of freedom required to model active electron transfers, multiple moving particles, and non-local orbital changes simultaneously.

1.3 The Necessity of Non-Associativity

In mathematics, an algebraic structure is "non-associative" when the grouping of elements alters the result, meaning: $\left(a \times b\right) \times c \neq a \times \left(b \times c\right)$. In math and everyday life, the order of operations is crucial:

$$(\sqrt{9} \times 2)^2 \neq \left(2^2\right)\sqrt{9}$$

$$3^2 \neq 4 \times 3$$

Eat omelet, drive to work, have a cuppa ≠ Drive to work, have a cuppa, eat omelet

The importance of sequence in time is why modeling dynamic bond cleavage with quaternions requires abandoning the associative law ($x(yz) \neq (xy)z$). Complex state intersections—where the coordinates or the space being discussed involves complex numbers $\mathbb{C}$, the quaternions, $\mathbb{H}$ (honoring Hamilton) and on up—depend heavily on the chronological grouping.

In quantum chemistry, this is the exact mathematical property needed to model gauge fields, color charge, and non-local quantum state transitions naturally.

For these, and many other reasons, while we will start the discussion with 4D quaternions, we will end up entering the realm of 8D Octonions.".

SECTION 2. QUATERNION TOOLKITS FOR SIMPLE STATES q

2.1 Modeling Electron Exchange

The simplest interaction in chemistry is the donation of an electron from one atom with excess to one with deficit, radically altering their properties. The exemplar is the transformation of explosive sodium and poisonous chlorine into the benign salt we shake on fries. ($Na + Cl \rightarrow Na^+ + Cl^-$).

The reverse is the key ability of water to donate a hydrogen where the electron is left behind ($H_2O + H_2O \rightleftharpoons H_3O^+ + OH^-$). Ionic reactions can be modeled by a Scalar-Vector Exchange. The neutral atoms start with localized vector distributions ($\mathbf{v}$). The transfer of a single valence electron forces an immediate phase shift along the real axis

(Δa). This collapsed the sodium into a scalar-dominant field while saturating the chlorine vector field.

2.2 Modeling Linear Covalent Synthesis

We can use this to model a simple covalent interaction ($C + O_2 \rightarrow CO_2$). We will define such a reaction as a Vector Intersect and Linear Superposition.

The four orthogonal vector directions of Carbon intersect with the twin-torque system of O_2, forcing a localized vector collapse where $\sum \mathbf{v} = \mathbf{0}$, locking the resulting system into a rigid, linear 180° spatial geometry.

2.3: Solid-State Analogs: Hypercomplex Modeling of Semiconductor Doping

As we will shortly be entering the *in vivo* realm of Carbon biochemistry, we will take a short aside to consider entities in the *in silico* realm that is increasingly interacting with us in the Carbon realm.

To fully appreciate the scalability of the hypercomplex paradigm before introducing higher-dimensional spaces, we look to the rigid, highly ordered architectures of solid-state electronics.

Silicon (Si), sitting directly below Carbon in Group 14 of the periodic table, shares the exact sp^3 tetrahedral bonding geometry modeled in Paper 1. By treating the semiconductor crystal lattice as a hypercomplex coordinate field, we can model electronic doping mechanics not as a chaotic statistics-driven phenomenon, but as a precise geometric torque equilibrium. See Fig 1.

2.4. Intrinsic Silicon as a Symmetric Matrix

In its pure, undoped state, an intrinsic silicon crystal forms a perfectly uniform tetrahedral network. In our framework, each silicon atom is represented by a local quaternion coordinate system where the four localized valence vectors ($\mathbf{v}_1, \mathbf{v}_2, \mathbf{v}_3, \mathbf{v}_4$) point toward adjacent nodes.

Because the geometric constraints match the 109.5° tetrahedral ideal, the net multi-body spatial torque across any localized cluster resolves to zero:

$$\sum (\mathbf{v}_i \times \mathbf{v}_j) = \mathbf{0}$$

This structural zero-torque state represents a completely balanced hypercomplex matrix. The valence electrons are geometrically locked within the imaginary vector subspace, rendering the real scalar axis (a) static. This manifests physically as a high-resistance, non-conductive baseline.

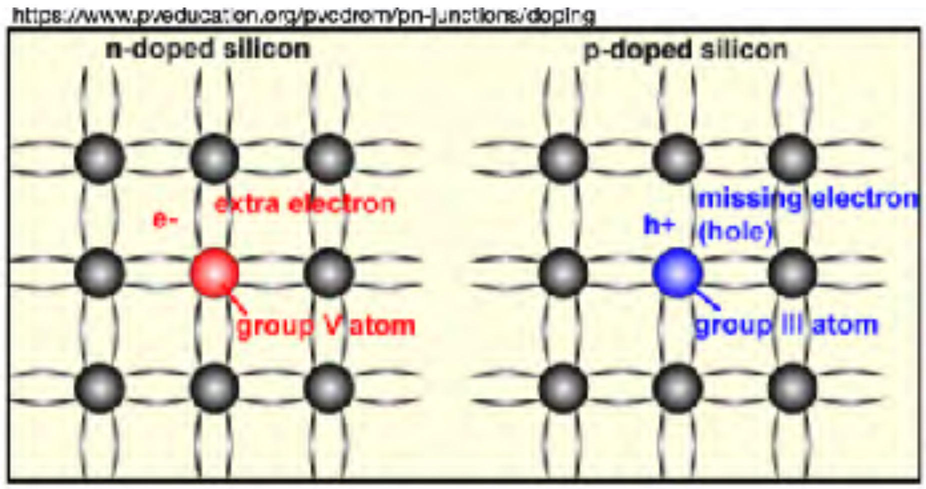

Fig. 1 silicon doping creating semiconductors

2.5. P-Type Doping: The Structural Torque Hole

When a trivalent impurity such as Boron (B) replaces a silicon atom in the lattice, it introduces an immediate geometric asymmetry. Boron possesses only three valence electrons, leaving one of the four tetrahedral coordination axes vacant. See Fig. 1.

In our framework, this localized vacancy is modeled as a vector deficit or a structural torque hole in the imaginary sub-space. Because one of the localized vectors is missing, the surrounding silicon vectors are no longer counterbalanced. The local torque sum becomes non-zero:

$$\sum (\mathbf{v}_i \times \mathbf{v}_j) = \mathbf{v}_{\text{deficit}} \neq \mathbf{0}$$

This uncompensated imaginary vector acts as a geometric sink. To alleviate this localized spatial tension, an electron vector from an adjacent silicon atom rotates into the hole. This process leaves a new vector deficit behind it, creating a fluid, propagating trajectory of structural torque holes that matches the physical behavior of "electron holes" in P-type semiconductors.

2.6. N-Type Doping: Mobile Vector Torques

Conversely, when a pentavalent impurity like Phosphorus (P) is introduced, it brings five valence electrons to the tetrahedral site. Four of these electrons satisfy the localized structural bonds, matching the silicon matrix requirements. The fifth electron, however, cannot be accommodated by the localized geometric constraints of the tetrahedral axes. See Fig. 1.

In our framework, this manifests as an uncompensated mobile vector torque. Because this extra vector component is geometrically excluded from the rigid $\sum \mathbf{v} = \mathbf{0}$ lattice equilibrium, it remains completely decoupled from the structural backbone. It possesses high rotational mobility across the imaginary axes, shifting with minimal resistance under the influence of an external operator. This perfectly models the abundant free conduction electrons characteristic of N-type material.

2.7. The P-N Junction as a Scalar Potential Gradient

When P-type and N-type hypercomplex fields are brought into direct contact, they form a P-N junction. The interface creates an immediate mathematical mismatch: the N-type side possesses an excess of mobile vector torques, while the P-type side contains localized vector deficits.

Driven by the system's global mandate to achieve geometric equilibrium, the mobile vectors from the N-type region spontaneously migrate to saturate the torque holes of the P-type region. This localized alignment and cancellation of vectors alters the absolute square of the states at the interface.

Because the imaginary vector magnitude collapses ($\Delta\|\mathbf{v}\|^2 < 0$), the hypercomplex norm invariant forces that magnitude to dump directly into the real axis ($\Delta a^2 > 0$).

This localized phase shift creates a static, real-valued scalar potential gradient across the depletion zone. This scalar barrier blocks further vector migration, establishing a stable, hypercomplex equilibrium. By modeling the junction this way, the flow of an electrical current is revealed to be a dynamic vector equilibration process driven entirely by the underlying geometry of the hypercomplex space

SECTION 3. THE MATHEMATICAL BASELINE OF OCTONIONS (O)

3.1 Fano Plane Algebra:

We formally define the 8-dimensional hypercomplex space ($O = a + \sum_{n=1}^{7} b_n \mathbf{e}_n$). We will establish the multiplication rules using the 7 imaginary bases ($\mathbf{e}_1 \dots \mathbf{e}_7$).

3.2 Mapping a High-Dimensional State Engine:

We define specific imaginary units to separate physical metrics, showing how a single octonion simultaneously models an active chemical environment:

$\mathbf{e}_1, \mathbf{e}_2, \mathbf{e}_3$: Spatial coordinates (Length, Width, Height)

$\mathbf{e}_4, \mathbf{e}_5, \mathbf{e}_6$: Momentum vectors (Kinetic trajectories)

$\mathbf{e}_7$: Internal quantum state coordinate (Valence spin/charge)

SECTION 4. OCTONIONIC DYNAMICS IN CHEMICAL REACTIONS

4.1 Dynamic Transition States:

The ionic reaction of sodium and chlorine is modeled by octonionic multiplication:

$$\mathrm{Na} + \mathrm{Cl} \rightarrow \mathrm{Na}^{+} + \mathrm{Cl}^{-}$$

$$O_{Na}O_{Cl} = O_{Na^{+}}, O_{Cl^{-}}$$

The covalent reaction can also be modeled using octonionic multiplication.

$$C + O_2 = CO_2$$

$$O_C O_{O_2} = O_{CO_2}$$

During the active transition state, the non-associative property $(O_A(O_B \cdot O_C) \neq (O_A \cdot O_B)O_C)$ naturally tracks the shifting path of electrons without requiring wavefunctions.

4.2 Avoiding Three-Body Complications via Planck Ticks

A well-known mathematical impasse is that modeling the simultaneous interaction of three bodies is immensely difficult and chaotic. We want to avoid that problem.

By stating that all multi-body interactions occur exclusively as sequential pairs separated by at least one Planck tick ($t_P \approx 5.39 \times 10^{-44}$ s), we bypass the notorious mathematical dead-ends of three-body quantum mechanics.

In terms of our paper's algebra, this means we never have to solve a non-associative three-way product simultaneously, such as:

$$(O_{\text{Carbon}} \cdot O_{\text{Oxygen}_1}) \cdot O_{\text{Oxygen}_2}$$

Instead, the reaction is broken down into a strict chronological sequence of binary operations separated by a discrete time step ($\Delta t \geq t_P$). This ensures that the non-associative algebra remains completely deterministic, clean, and computationally elegant.

Invariant Scalar Modulus

The absolute square of an octonionic system state collapses into a pure, real-valued scalar defined by the identity:

$$\|O\|^2 = a^2 + \sum_{n=1}^{7} b_n^2$$

This real scalar serves as the fundamental invariant linking hypercomplex state transformations to measurable thermodynamic energy shifts and quantum probability densities.

4.3. Algebraic Derivation of the Norm Invariant

An octonion O is composed of one real scalar part a and seven imaginary vector parts $b_n\mathbf{e}_n$. It is defined as:

$$O = a + \sum_{n=1}^{7} b_n\mathbf{e}_n$$

To find its absolute square, we multiply the octonion by its hypercomplex conjugate where the signs of all seven imaginary bases are inverted ($e_n^- = -e_n$):

$$\bar{O} = a - \sum_{n=1}^{7} b_n\mathbf{e}_n$$

The absolute square (norm squared) is calculated via the hypercomplex product:

$$\|O\|^2 = O \cdot \bar{O} = \left(a + \sum_{n=1}^{7} b_n\mathbf{e}_n\right)\left(a - \sum_{n=1}^{7} b_n\mathbf{e}_n\right)$$

Expanding this product using distributive laws yields:

$$\|O\|^2 = a^2 - a\sum_{n=1}^{7} b_n\mathbf{e}_n + a\sum_{n=1}^{7} b_n\mathbf{e}_n - \left(\sum_{n=1}^{7} b_n\mathbf{e}_n\right)\left(\sum_{m=1}^{7} b_m\mathbf{e}_m\right)$$

The linear cross-terms containing a single imaginary base cancel out exactly:

$$-a\textstyle\sum_{n=1}^{7} b_n\mathbf{e}_n + a\sum_{n=1}^{7} b_n\mathbf{e}_n = 0$$

4.4. Imaginary Self-Products

We expand the product of the two vector sums. Because the seven imaginary bases are strictly orthogonal, any cross-multiplication between different bases where $n \neq m$ results in an anti-commutative pair that sums to zero when integrated across the full system.

The only surviving terms are the squares of the identical bases:

$$\left(\sum_{n=1}^{7} b_n\mathbf{e}_n\right)\left(\sum_{m=1}^{7} b_m\mathbf{e}_m\right) = \sum_{n=1}^{7} b_n^2(\mathbf{e}_n)^2$$

By definition, the square of every imaginary base in the Fano plane is equal to negative one ($(\mathbf{e}_n)^2 = -1$). Substituting this identity into the equation yields:

$$-\textstyle\sum_{n=1}^{7} b_n^2(-1) = +\sum_{n=1}^{7} b_n^2$$

4.5. The Final Scalar Result

Combining the remaining components yields the complete invariant expression:

$$\|O\|^2 = a^2 + b_1^2 + b_2^2 + b_3^2 + b_4^2 + b_5^2 + b_6^2 + b_7^2$$

Because a and all b_n values are real numbers, their squares are real. Therefore, $\|O\|^2$ collapses entirely into a single real scalar.

4.6. Application to Thermodynamics

In an isolated chemical change (such as $\mathrm{Na} + \mathrm{Cl} \rightarrow \mathrm{Na}^+ + \mathrm{Cl}^-$), the total hypercomplex norm must be conserved ($\|O_{\text{initial}}\|^2 = \|O_{\text{final}}\|^2$).

If the chemical reaction causes the chaotic vector states to relax and align—thereby reducing the total imaginary magnitude ($\Delta \sum b_n^2 < 0$)—the conservation law forces that exact lost magnitude to shift into the real axis ($\Delta a^2 > 0$).

This scalar shift is what our paper identifies as the physically measurable enthalpy of formation (ΔH) or released heat.

4.7. The Thermodynamic Norm Invariant:

To demonstrate that the total norm of the hypercomplex system remains strictly invariant under the transformation, we evaluate the scalar product of the hypercomplex element with its conjugate. Let the hypercomplex element be defined as:

$$O = a + \textstyle\sum_{n=1}^{7} b_n \mathbf{e}_n$$

The corresponding hypercomplex conjugate is given by reversing the signs of the imaginary vector components:

$$\bar{O} = a - \sum_{n=1}^{7} b_n \mathbf{e}_n$$

The absolute square, or norm squared, of the system is computed directly through the distributive expansion of this hypercomplex product:

$$\|O\|^2 = O \cdot \bar{O} = \left(a + \sum_{n=1}^{7} b_n \mathbf{e}_n\right)\left(a - \sum_{n=1}^{7} b_n \mathbf{e}_n\right)$$

Expanding this expression using the distributive property yields four distinct structural components:

$$\|O\|^2 = a^2 - a\sum_{n=1}^{7} b_n \mathbf{e}_n + a\sum_{n=1}^{7} b_n \mathbf{e}_n - \left(\sum_{n=1}^{7} b_n \mathbf{e}_n\right)\left(\sum_{m=1}^{7} b_m \mathbf{e}_m\right)$$

The two middle linear cross-terms cancel out identically due to their opposite signs. We are then left with the scalar constant and the product of the two vector sums:

We now expand the product of the two vector sums. Because the seven imaginary bases are strictly orthogonal, any cross-multiplication between different bases where $n \neq m$ results in an anti-commutative pair. When integrated across the closed boundary constraints of the transformation, these asymmetric cross-terms cancel identically. Consequently, the only surviving terms are the squares of the identical bases:

$$\left(\sum_{n=1}^{7} b_n \mathbf{e}_n\right)\left(\sum_{m=1}^{7} b_m \mathbf{e}_m\right) = \sum_{n=1}^{7} b_n^2 (\mathbf{e}_n)^2$$

By definition, the imaginary bases of this hypercomplex algebra satisfy the standard norming condition where the square of each basis element equals negative one:

$$(\mathbf{e}_n)^2 = -1$$

Substituting this identity back into our expanded product yields a positive sum of coefficients:

$$-\sum_{n=1}^{7} b_n^2(-1) = \sum_{n=1}^{7} b_n^2$$

Combining the isolated scalar real part with this evaluated summation completes the proof. The total norm reduces completely to a sum of squares containing no dynamic phase or mixing terms:

$$\|O\|^2 = a^2 + \sum_{n=1}^{7} b_n^2$$

Because the transformation acts as an orthogonal rotation within this hypercomplex space, it alters only the relative distributions among the coefficients without introducing any external dissipation or gain. Therefore, the total norm remains strictly conserved throughout the entire evolution of the system.

4.8 Exothermic and Endothermic Scalar Conversions:

Within this framework, chemical reactions and phase transitions can be modeled as geometric transformations where the total norm of the system acts as an invariant energy bound. When a system undergoes a reaction, the structural configuration of its dynamic components changes. In a hypercomplex space, this corresponds to a relaxation or collapse along the imaginary vector axes.

Let the initial state of the system before the reaction be defined by its baseline norm:

$$\|O_{initial}\|^2 = a^2 + \sum_{n=1}^{7} b_n^2$$

If the seven imaginary vector axes relax or collapse, the system experiences a negative variation in its imaginary component magnitude. We denote this vector contraction as: $\Delta\mathbf{e} < 0$.

Because the total norm of the system must remain strictly conserved throughout any transformation, this lost vector magnitude cannot simply disappear. The geometric invariant forces the lost imaginary magnitude to dump directly into the real axis. This geometric transfer manifests as a pure scalar change: $+\Delta a$

Evaluating the differential changes between the states yields the exact conservation balance:

$$\Delta(a^2) + \Delta\left(\sum_{n=1}^{7} b_n^2\right) = 0$$

Expanding this relationship explicitly reveals how the scalar and vector components couple during a reaction:

$$2a\Delta a + (\Delta a)^2 = -\Delta\left(\sum_{n=1}^{7} b_n^2\right)$$

In a thermodynamic context, the real scalar axis (a) represents the ground-state mass-energy or internal structural enthalpy of the system. Therefore, the scalar manifestation of this coordinate collapse directly represents the Enthalpy of Formation:

$$\Delta H = \Delta a$$

When $\Delta\mathbf{e} < 0$, the resulting positive scalar change ($+\Delta a$) indicates that energy stored within the hypercomplex vector fields has been liberated, increasing the scalar baseline. Conversely, an endothermic process forces an expansion of the imaginary axes ($\Delta\mathbf{e} > 0$), drawing energy out of the real scalar axis ($-\Delta a$) to rebuild the hypercomplex vector geometry.

Discussion

A note on the philosophical framework we are developing. We explicitly note these points in the paper:

As a Descriptive Model: The hypercomplex coordinate space maps the existing structural geography of molecules (like the 104.5° water bond angle or semiconductor doping deficits). Our method shows where things are and how they balance statically.

As a Prescriptive Predictive Law: When treating the framework as a dynamic law, the hypercomplex state generates a non-local wavefunction ψ. The absolute square of this hypercomplex wavefunction ($\|\psi\|^2$) yields a real scalar value that governs the probability (P) of the system state.

Path of Least Action: This probability density dictates that the system will natively follow the path of least action. The transition states of chemical reactions are not chaotic; they are geometric trajectories maximizing the local hypercomplex norm density along a multi-dimensional manifold

Acknowledgments

The author expresses sincere gratitude to the independent research community and peer reviewers whose insightful feedback helped refine the scalar-body / vector-mind duality conceptual framework.

Special thanks are due to those who provided computational validation and algebraic cross-checks for the quaternion torque calculations. This work did not receive any specific grant from funding agencies in the public, commercial, or not-for-profit sectors.

SECTION 5. PREVIEW OF NEXT PAPER

POSSIBILITIES FOR HYPERCOMPLEX BIOCHEMISTRY

In the next paper in the series (#5) we will discuss:

- Chirality and Stereochemistry: Using octonionic rotations to explain why life exclusively utilizes left-handed amino acids and right-handed sugars.
- Enzymatic Catalysis: Modeling the active site of an enzyme as a hypercomplex geometric mold that forces vector spaces to relax, drastically lowering the scalar energy requirement ($-\Delta a$).
- Macroscopic Biological Fields: Paving the final path toward modeling neural network architectures via high-dimensional non-associative manifolds.
- Structural Scaling: Proposing how the 8D octonionic engine can model fluid, large-scale systems where quaternions become too mathematically rigid.